Biomedicine & Pharmacotherapy 139 (2021) 111611

Contents lists available at ScienceDirect

Biomedicine & Pharmacotherapy

journal homepage: www.elsevier.com/locate/biopha

Modulation of peptidases by 2,4-diamine-quinazoline derivative induces cell death in the amitochondriate parasite *Trichomonas vaginalis*

Juliana Inês Weber [a], Graziela Vargas Rigo [a], Débora Assumpção Rocha [b], Isadora Serraglio Fortes [b], Adriana Seixas [c,d], Saulo Fernandes de Andrade [b], Tiana Tasca [a,*]

[a] Faculty of Pharmacy and Centre of Biotechnology, Federal University of Rio Grande do Sul, Porto Alegre, RS, Brazil
[b] Pharmaceutical Synthesis Group (PHARSG), Faculty of Pharmacy, Federal University of Rio Grande do Sul, Porto Alegre, RS, Brazil
[c] Department of Pharmacosciences, Federal University of Health Sciences of Porto Alegre, Porto Alegre, RS, Brazil
[d] National Institute of Science and Technology in Molecular Entomology, Brazil

ARTICLE INFO

Keywords:
Trichomonas vaginalis
Amitochondriate
Quinazoline
Cell death
Peptidases

ABSTRACT

Trichomonas vaginalis is an amitochondriate protozoan and the agent of human trichomoniasis, the most prevalent non-viral sexually transmitted infection (STI) in the world. In this study we showed that 2,4-diamine-quinazoline derivative compound (PH100) kills *T. vaginalis*. PH100 showed activity against fresh clinical and American Type Culture Collection (ATCC) *T. vaginalis* isolates with no cytotoxicity against cells (HMVI, 3T3-C1 and VERO) and erythrocytes. In addition, PH100 showed synergistic action with metronidazole, indicating that these compounds act by different mechanisms. When investigating the mechanism of action of PH100 to ATCC 30236, apoptosis-like characteristics were observed, such as phosphatidylserine exposure, membrane alterations, and modulation of gene expression and activity of peptidases related to apoptosis. The apoptosis-like cell death features were not observed for the fresh clinical isolate treated with PH100 revealing distinct profiles. Our data revealed the heterogeneity among *T. vaginalis* isolates and contribute with the understanding of mechanisms of cell death in pathogenic eukaryotic organisms without mitochondria.

1. Introduction

The sexually transmitted infections (STIs) are a public health problem. Despite the incentive for protection, there are still many barriers for an efficient fighting line to be established. One of the contributing factors for the high number of cases is the lack of access to quick and accurate diagnosis of some STIs by the population of low-income countries [1]. Among STIs, trichomoniasis is not of compulsory notifying which contributes for an underestimated number of cases [2]. In 2016 the numbers of cases among adults infected by non-viral STIs – *Chlamydia trachomatis*, *Neisseria gonorrhoeae*, syphilis and *Trichomonas vaginalis* – reached 376.4 million, being *T. vaginalis* responsible for 156 million of cases and for the highest prevalence and incidence in the world [3]. A study shows that 80% of cases of trichomoniasis are asymptomatic in women and men, a fact that potentiate the disease risk of transmission [4]. Beyond the problems derived from trichomoniasis, including increased risk of cervical and prostate cancers, problems during pregnancy, pelvic inflammatory disease, infertility, the infection is a cofactor of transmission and acquisition of HIV [5–7].

The only class of drugs approved for the treatment of trichomoniasis is 5-nitroimidazoles, with metronidazole as first choice, and tinidazole. The mechanism of action of metronidazole is not completely elucidated. The drug enters the trophozoite by passive diffusion and the nitro group is chemically reduced in the hydrogenosome (the organelle by which trichomonads generate ATP as they do not have mitochondria) or in the cytosol generating nitro-radical anions, which are toxic to the parasite. Treatment with metronidazole occasionally causes side effects such as nausea, vomiting, diarrhea, abdominal discomfort, and hypersensitivity [8]. In addition, there is estimative of up to 10% of cases being non-responsive to treatment and the resistance to metronidazole is estimated in 2–10% of cases, eliciting the necessity of new therapeutic options [9,10].

Quinazoline is composed by two aromatic rings fused by six members, benzene and pyrimidine [11]. The interest for the quinazoline has been intensified by discovery of febrifugine, which presents antimalarial activity [11]. The FDA (Food and Drug Administration) has approved many derivatives as anticancer drugs, such as the gefitinib, erlotinib, and lapatinib [11]. Moreover, studies have already shown that

* Correspondence to: Federal University of Rio Grande do Sul, Av. Ipiranga, 2752, 90610-000 Porto Alegre, RS, Brazil.
E-mail address: tiana.tasca@ufrgs.br (T. Tasca).

https://doi.org/10.1016/j.biopha.2021.111611
Received 20 November 2020; Received in revised form 29 March 2021; Accepted 12 April 2021
Available online 28 May 2021

derivatives of quinazoline present pharmacological activities: anti-inflammatory [12], anticancer [13], against multi-resistant *Staphylococcus aureus* [14], antibacterial and antibiofilm of *S. aureus* and *S. epidermidis* [15], anti-*Leishmania* [16], anti-*Trypanosoma* [16], anti-malaric [17], for Alzheimer treatment [18], antimicrobial [19], anti-hyperglicemic [20], anticonvulsant [21], antidepressant [22] and anti-hypertensive [23].

Based on previous studies that reveal the biological activities of quinazoline and that *T. vaginalis* is considered a model in cellular biology to study mechanisms of cell death regarding the feature of being amitochondriate, in this study we demonstrated that the 2,4-diamine-quinazoline derivative kills *T. vaginalis*. The mode of action includes the modulation of peptidases and revealed distinct profiles of cell death related to *T. vaginalis* isolate type.

2. Materials and methods

2.1. 2,4-diamine-quinazoline derivative synthesis

PH100 (N^4-benzyl-N^2-phenylquinazoline-2,4-diamine) was synthesized as previously described [15]. Briefly, the 4-Cl of the commercially available 2,4-dichloroquinazoline was replaced by benzylamine and next the 2-Cl was replaced by aniline (Scheme 1).

2.2. Chemical characterization of PH100

The chemical characterization of PH100 was determinate by ^{1}H and ^{13}C nuclear magnetic resonance (NMR), mass spectrometry (MS), and infrared (IR) analyses (Supplemental Figs. S1A and B, S2 and S3). The compound PH100 is a yellow solid, obtained in 81% yield. M.p: 142–145 °C. IR (ν/cm^{-1}): 3431, 3027, 1568, 1485, 1415, 1326. ^{1}H NMR (400 MHz, DMSO-d_6) δ 9.02 (s, 1 H), 8.68 (t, 1 H, J = 5.4 Hz), 8.16 (d, 1 H, J = 8.0 Hz), 7.84–7.82 (m, 2 H), 7.60 (t, 1 H, J = 8.0 Hz), 7.44–7.40 (m, 3 H), 7.33 (t, 2 H, J = 7.4 Hz), 7.25–7.18 (m, 4 H), 6.86 (t, 1 H, J = 7.2 Hz), 4.83 (d, 2 H, J = 5.4 Hz). ^{13}C NMR (100 MHz, DMSO-d_6) δ 160.1, 156.9, 151.4, 141.4, 139.7, 132.6, 128.3, 127.1, 126.7, 125.3, 122.8, 121.5, 120.4, 118.5, 111.6, 43.5. HRMS (m/z): [MH+] calc for C21H19N4, 327.1604; found, 327.1604.

2.3. Culture of T. vaginalis

In the assays *T. vaginalis* ATCC 30236 isolate and three fresh clinical isolates (TV-LACH4, TV-LACM15 and TV-LACM22) were used. The isolates were selected according: harboring TVV (*Trichomonasvirus*) only (TV-LACH4), *Mycoplasma hominis* only (TV-LACM22), *M. hominis* and TVV (ATCC 30236), or not harboring TVV neither *M. hominis* (TV-LACM15). Trophozoites were cultured *in vitro* at 37 °C in trypticase-yeast extract-maltose (TYM) medium, supplemented with 10% (vol/vol) heat inactivated bovine serum [24]. Parasites in the logarithmic phase of growth were centrifuged and resuspended on new TYM medium for anti-*T. vaginalis* assays.

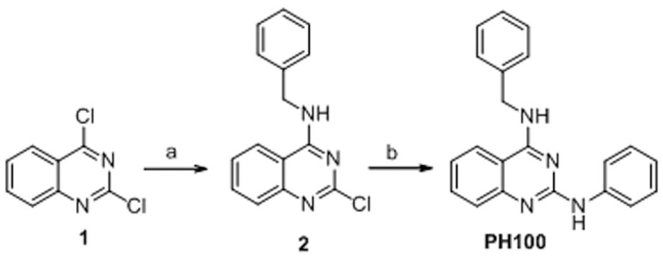

Scheme 1. Synthetic procedures to obtain PH100 (N^4-benzyl-N^2-phenylquinazoline-2,4-diamine). *Reagents and conditions:* (a) benzilamine, sodium acetate, THF: H_2O, 65 °C; (b) aniline, EtOH, 120 °C. 2,4-dichloroquinazoline (**1**) and N-benzyl-2-chloroquinazolin-4-amine (**2**).

2.4. Minimum inhibitory concentration (MIC) and IC_{50} determination

The MIC and the IC_{50} values for PH100 anti-*T. vaginalis* activity were determined on 96-well microtiter plates, where different volumes of TYM medium were added to each well. PH100 at eight-fold serial dilution from 100 μM and 1.0 × 10^5 trophozoites/mL were incubated at 37 °C, 5% CO_2 for 24 h. Three controls were used: trophozoites with no treatment, the vehicle control (DMSO 0.6%), and the positive control with 100 μM metronidazole. After incubation, the parasites were counted using hemocytometer and analyzed for their motility and morphology by trypan blue exclusion dye (0.2%, vol/vol). The wells corresponding to MIC values and concentrations below and above, as well as controls were inoculated in fresh TYM medium at 37 °C. The parasites were analyzed every 24 h for 120 h to confirm MIC. The results were expressed as the percentage of viable trophozoites compared to negative control.

2.5. In vitro cytotoxicity assay

The non-tumor murine fibroblast lineage, 3T3-C1, a non-tumor lineage from kidney epithelium, VERO, and a tumor lineage from human vaginal epithelium, HMVII, were used. 3T3-C1 and VERO were cultured in DMEM medium and HMVII in RPMI medium both supplemented with 10% fetal bovine serum (FBS) and incubated at 37 °C, 5% CO_2. For the test, 1.0 × 10^4 cells/well were seeded in 96-well microtiter plates for 24 h. After, the medium was replaced with fresh medium containing PH100 at serial dilutions from 100 μM. Three controls were used: control with cells only, vehicle control (DMSO 0.6%) and positive control (Triton X-100 0.2%). The plates were incubated for 48 h. After this time, a solution of 3-(4,5-dimethylthiazol-2-yl)−2,5-diphenyltetrazolium bromide (MTT) (0.5 mg/mL) was added and incubated for 1 h at 37 °C. MTT was removed and the insoluble purple formazan was dissolved in DMSO. The amount of reduced MTT was measured at 570 nm [25].

2.6. In vitro hemolytic assay

Erythrocytes were obtained from the heparinized blood of healthy human donors. The UFRGS Research Ethical Committee approved documents, procedures, and project under authorization CAAE 47423415.5.0000.5347. Erythrocytes suspension (5 × 10^7 cells/mL) was incubated with PH100 at decreasing concentrations from 100 μM, for 24 h at 37 °C [26]. Three controls were prepared: control with erythrocytes only, vehicle control (DMSO 0.6%) and positive control (Triton X-100 0.2%). Hemoglobin released into the supernatants was quantified spectrophotometrically at 540 nm.

2.7. Effect of PH100 compound in T. vaginalis kinetic growth assay

The *T. vaginalis* ATCC 30236 and the fresh clinical isolate TV-LACM15 were treated or not with PH100 at a density of 1.0 × 10^5 trophozoites/mL (including vehicle control and control with parasites only) at the MIC and IC_{50} values and incubated in TYM medium. The counting of viable trophozoites with hemocytometer was performed at 2, 4, 6, 12, 24, 48, 72, 96 and 120 h. The results were expressed as trophozoites/mL by comparing treated viable trophozoites with untreated parasites.

2.8. Checkerboard assay

The *T. vaginalis* TV-LACM15, TV-LACM22 and TV-LACH4 isolates were used in this assay due to their lowest susceptibility to metronidazole when comparing to the tested ATCC in this study. In order to check metronidazole and PH100 interaction, both compounds were tested at concentrations: 4 x IC_{50}, 2 x IC_{50}, IC_{50}, ½ x IC_{50}, ¼ x IC_{50}. Two controls were used: control containing trophozoites with no treatment and

vehicle control. Fractional inhibitory concentration index (FICI) was estimated using the following formula: FICA + FICB = FICI, where FICA is the value of PH100 in the combination/value of PH100 alone, and FICB is the value of metronidazole in the combination/value of metronidazole alone. The interaction was classified as 'synergy' if FICI $\leq$ 0.5, 'no interaction' if FICI = 0.5–4.0 and 'antagonism' if FICI > 4.0 [27].

2.9. Quantification of reactive oxygen species (ROS) production by T. vaginalis

Some modifications were carried out to the method previously described [28]. Trophozoites of ATCC 30236, TV-LACM15, TV-LACM22 and TV-LACH4 isolates were washed with phosphate buffered saline 1x (PBS pH 7.0; 37 °C), resuspended at 5.0×10^6 trophozoites/mL density with 2′,7′-dichlorofluorescein diacetate (2′,7′-DCF-DA) in a final concentration of 10 μM and incubated for 1 h at 37 °C. After, PH100 or metronidazole was added to the isolates at their respective IC_{50} values and incubated for 1 h. Two controls were used: trophozoites with no treatment and positive control (parasites treated with 5.0 mM of hydrogen peroxide). The production of ROS was evaluated through fluorescence measured by flow cytometry (FACSVerse, Becton Dickinson, CA) and 10,000 cells were gated and analyzed using the FACSuite ™ software (Becton Dickinson).

2.10. Annexin V-FITC assay

Trophozoites (ATCC 30236 and TV-LACM15 isolates) were treated with PH100 at the IC_{50} for 24 h, were washed with PBS 1x (pH 7.0; 37 °C), resuspended in binding buffer, resulting in a concentration of 1.0×10^6 trophozoites/mL. Then, 100 μL of parasite suspension, 5 μL of Annexin V-FITC, and 5 μL of propidium iodide (PI) were added to the incubation media at 25 °C for 15 min (protected from light) and after, 100 μL of binding buffer added. Apoptosis was measured by flow cytometry (FACSVerse, Becton Dickinson, CA) and 10,000 trophozoites were gated and analyzed using FACSuite™ software (Becton Dickinson).

2.11. Determination of autophagy by acridine orange

Acridine orange is a cell-permeable green fluorophore that can be protonated and trapped in acidic vesicular organelles, such as autolysosomes, where it shifts to red fluorescence. This makes acridine orange staining a quick, accessible and reliable method to assess autophagy induction [29]. Trophozoites (ATCC 30236 and TV-LACM15 isolates) treated with PH100 at the IC_{50} for 24 h, were washed and resuspended with DMEM. 100 μL of 1.0×10^6 trophozoites with 1.0 μg/mL of acridine orange were incubated at 25 °C for 15 min. Autophagy was measured by flow cytometry (FACSVerse, Becton Dickinson, CA) and 10,000 trophozoites were gated and analyzed using FACSuite™ software (Becton Dickinson).

2.12. Effect of PH100 on gene expression of T. vaginalis enzymes

In order to investigate the involvement of enzymes related to apoptosis in the mechanism of action of PH100, the gene expression of six enzymes was analyzed by Real-Time qRT-PCR. The ATCC 30236 isolate and the fresh clinical isolate TV-LACM15 were incubated for 24 h with PH100 at IC_{50} values. After incubation, total mRNA was extracted with TriZol™, the purity and quantity were measured on the Thermo Scientific NanoDrop 1000® spectrophotometer and only high-quality samples were used on the analysis. Standard curve primers were performed using cDNA in 0.1 mL strip tubes using GoTaq® 1-step RT-qPCR system. For analyzes, reaction tubes contained a final volume of 12 μL: 5 μL 2x GoTaq® qPCR Master Mix, 0.2 μL GoScript ™ RT Mix, 0.1 or 0.2 μM primer and 2 μL RNA. ID genes were obtained in previous apoptosis studies with other cell lines. The search of homolog enzymes in *T. vaginalis* were obtained on TrichDB (https://trichdb.org/trichdb/) and sequences were chosen considering lower similarity with human genes. These sequences were used to design primers in Primer 3plus (http://www.bioinformatics.nl/cgi-bin/primer3plus/primer3plus.cgi) and aligned against the *T. vaginalis* genome to verify their specificity (Supplemental Table S1). Quantitative reverse transcriptions were performed using 5 ng of RNA and cycling conditions were enzyme activation at 95 °C for 10 min followed by 40 cycles: 95 °C for 10 s; 60 °C, 64 °C or 68 °C for 40 s with fluorescence collection and the final step of 72 °C for 40 s. Melting curve was performed by increasing temperature from 60 °C, 64 °C and 68 °C to 95 °C with 1 °C for 5 s. DNA topoisomerase II (*DNAtopII*) was used as normalizing gene and reactions were performed as previously described [30]. Negative control with no mRNA was used. Rotor-Gene Q series software 2.1.0 were used to analyze of mRNA relative expression of genes. DNA topoisomerase II (*DNAtopII)* gene value (ΔCt) was used for threshold cycles (Ct) and sample was compared to control (ΔΔCt). Fold change values were expressed as $2^{-\Delta\Delta Ct}$.

2.13. Scanning electron microscopy (SEM)

Trophozoites (ATCC 30236 isolate that presented morphological alterations observed by SSC and FSC) were treated or not with PH100 at IC_{50} for 24 h, washed with PBS 1x and fixed in 2.5% (vol/vol) glutaraldehyde for 2 h 30 min. Then, organisms were washed with sodium cacodylate buffer (0.1 M pH 7.2) and post-fixed in 1% (vol/vol) osmium tetroxide for 2 h. The samples were added on a circular cover slip and dehydrated in acetone gradient (30, 50, 70, 80, 95 and 100º GL). Critical point dried was carried out with CO_2 and coated with gold particles. Samples were observed in JEOL JSM 6060 scanning electron microscope.

2.14. Peptidases activity by azocasein assay

Azocasein degradation assay was used to verify the effect of PH100 on peptidases activity. Protein levels were measured using the Bradford method [31] and a final concentration of 0.8 mg/mL was used to assure linearity in 0.1 M Tris-HCl pH 7.0. The assay was carried out for 90 min at 37 °C with 2.0% azocasein (Sigma-Aldrich, Co.) as substrate. The reaction was interrupted with cold 10% trichloroacetic acid. The samples were centrifuged at 10,000*g* for 5 min and 1.8 N NaOH was added to supernatants. Absorbance was measured at 420 nm. Percentage of azocasein degradation was compared between the control as non treated parasites showing 100% of peptidase activity and trophozoites PH100-treated at IC_{50}.

2.15. Peptidases zymograms and mass spectrometry analysis

Peptidase activities were analyzed using SDS-PAGE on 12.5% polyacrilamide gel co-polymerized with 1.0% gelatin. After 24 h of incubation with PH100 at IC_{50} (ATCC 30236 and TV-LACM15) trichomonads were washed with 0.8% saline. Total protein levels were measured using the Bradford method [31] and the final concentrations were adjusted with sample buffer (H_2O, 0.5 M Tris-HCl pH 6.8, glycerol, 10% SDS and bromophenol) to 0.06 mg/mL protein. After electrophoresis, peptidases were renatured with 2.5% Triton X-100 for 1 h and activated with 50 mM phosphate buffer pH 5.5 for 24 h at 37 °C. Gel was washed with water and stained with Comassie brilliant blue for 2 h to determine proteolytic activity that was detected as white bands against a blue background after destaining with 40% methanol in 10% acetic acid. Both *T. vaginalis* isolates with no treatment were used as negative controls. In addition, SDS-PAGE on 12.5% polyacrilamide gel was carried out without gelatin to approximately determinate the molecular weight of protein bands.

Peptidases activity regions were cut off the zymogram and the gel digestion was performed using 50 mM ammonium bicarbonate and

acetonitrile. The gel pieces were dehydrated with 100% acetonitrile and lyophilized. The reduction was done using 50 mM dithiothreitol in 50 mM ammonium bicarbonate, for 30 min at 56 °C. Then, alkylation with 50 mM iodoacetamide in 50 mM ammonium bicarbonate for 30 min, at room temperature, was carried out. 50 mM ammonium bicarbonate and 40% acetonitrile were added to the gel pieces for 15 min and a second dehydration step was done. Proteins were digested in 100 mM ammonium bicarbonate solution containing 100 ng of sequencing grade trypsin (Promega) for 16 h at 37 °C. Supernatants were transferred to new microtubes and the gel pieces were washed with 1.0% formic acid in 60% acetonitrile and the solution was transferred to new microtubes. Finally, digested peptides were lyophilized and resuspended in 0.1% formic acid and 5 μL of each solution were subjected to reversed phase chromatography (Nano Acquity Ultra Performance LC-UPLC® chromatograph, Waters) using a Nanoease C18, 75 μm ID at 35 °C. The column was equilibrated with 0.1% trifluoroacetic acid and the peptides were eluted in a 20 min gradient, ramping from 0% to 60% acetonitrile in 0.1% TFA at 0.6 nL/min constant flow. Eluted peptides were lyophilized and analyzed by mass spectrometry using a G2-XS Q-TOF Xevo® spectrometer. Protein identification was performed using ProteinLynx Global SERVER Version 3.0.3. The central analytical platform for Waters proteomics systems. The protein identification was performed using a databank of *T. vaginalis* genome data (*T. vaginalis* G3; ATCC PRA-98, WGS project AAHC01000000 data) [32].

2.16. Statistical analysis

All experiments were performed in triplicate and with at least three independent cultures (n = 3). Data were expressed by mean ± standard deviation (S.D.). Statistical analysis was conducted using the Student's *t*-test and a 5% level of significance was applied to the data. The GraphPad Prism software (San Diego, CA) was used for IC_{50} and CC_{50} determination by non-linear regression. The selectivity index (SI) for each mammalian cell was calculated based on the ratio CC_{50}/IC_{50}.

3. Results

3.1. PH100 killed T. vaginalis, presented low cytotoxicity and no hemolytic effect

The compound PH100 was tested against fresh clinical isolates (TV-LACM15, TV-LACM22, and TV-LACH4) and ATCC 30236. The fresh clinical isolate TV-LACM15 was the most susceptible to PH100, with IC_{50} 14.8 μM. It is important to emphasize that TV-LACM15 was the most metronidazole resistant among the isolates tested. PH100 showed low values of HC_{50} and high SI against erythrocytes, indicating that compound was not hemolytic. In addition, PH100 revealed low cytotoxicity against mammalian cells with SI values higher than 1.0 (Table 1). The values of SI showed that PH100 was selective, exhibiting greater toxicity to the parasite than to the host cells.

3.2. PH100 abolished T. vaginalis growth

To analyze the influence of PH100 on *T. vaginalis* proliferation, kinetic growth experiments using ATCC 30236 and TV-LACM15 isolates were performed. An initial inoculum of 1×10^5 trophozoites/mL was incubated in the presence of PH100 at MIC and IC_{50} values and the results show the curve of viable trichomonads. The effect of PH100 at IC_{50} concentration caused a delay on trophozoites proliferation, as expected due to lower PH100 concentration, and organisms recovered growth after 48 h (Fig. 1A and C). Conversely, when tested at MIC, PH100 totally inhibited the parasite growth of both isolates after 6 h of incubation (Fig. 1B and D).

3.3. PH100 showed synergistic effect with metronidazole

The checkerboard assay showed a synergistic effect (FICI ≤ 0.5) at the highest metronidazole concentration (4 x IC_{50}, 4.22 μM) associated with PH100 at IC_{50} or higher concentrations to all fresh clinical isolates tested. The checkerboard assay was performed upon association of PH100 and metronidazole using TV-LACM15, TV-LACM22 and TV-LACH4 isolates (Fig. 2). These fresh clinical isolates presented lower metronidazole susceptibility when compared with ATCC 30236. For the TV-LACM22 and TV-LACH4 isolates, combinations starting from PH100 $IC_{50}/4$ with different concentrations of metronidazole have already shown a synergistic effect, with 100% death for TV-LACM22 (isobolograms in Supplemental Fig. S4).

3.4. PH100 did not affect ROS production by T. vaginalis

Addition of PH100 or metronidazole at IC_{50} did not significantly affect intracellular ROS production by any isolate tested when compared to hydrogen peroxide (positive control) (Supplemental Fig. S5).

3.5. PH100 induced apoptosis-like cell death only in the ATCC isolate

PH100 induced phosphatidylserine exposition in ATCC 30236 trophozoites suggesting an apoptosis-like cell death, revealing fluorescent units in characteristic regions (Fig. 3). On the other hand, and intriguing, PH100 did not induce cytoplasmatic translocation of phosphatidyserine after Annexin V assay in TV-LACM15 trophozoites, differing from the ATCC isolate. Table 2 demonstrated increase in granularity (FSC) and cell internal complexity (SSC) as amount and type of cytoplasmic granules and membrane roughness, suggesting morphological changes in ATCC 30236 trophozoites.

3.6. PH100 did not induce autophagy on T. vaginalis

No emission of red fluorescence on the flow cytometry was observed in both ATCC 30236 and TV-LACM15 isolates treated with PH100 at IC_{50} in 24 h in comparison to their respective controls with no treatment (Supplemental Fig. S6). This finding indicates that PH100 did not induce autophagy in *T. vaginalis*.

3.7. PH100 modulated gene expression of apoptosis-like enzymes

The quantification of gene expression of enzymes related to apoptosis was compared to the normalizing gene of DNA topoisomerase II. As shown in Fig. 4, when ATCC 30236 and TV-LACM15 trophozoites were treated with PH100 it was observed no significant changes in the gene expression of PARP for ATCC 30236, but a significant increase for the TV-LACM15 isolate was observed. The gene expression of cathepsin D-like (TvCatD) decreased in ATCC 30236 and increased in TV-LACM15 isolate. On the other hand, cathepsin B-like was increased, cathepsin L-

Table 1
Anti-*Trichomonas vaginalis* activity and cytotoxicity effect of PH100 and metronidazole. MIC and IC_{50} values express in μM.

Compound	ATCC 30236		TV LACM15		TV LACM22		TV LACH4		VERO		HMVII		3T3-C1		Erythrocytes	
	MIC	IC_{50}	MIC	IC_{50}	MIC	IC_{50}	MIC	IC_{50}	CC_{50}	SI	CC_{50}	SI	CC_{50}	SI	CC_{50}	SI
PH100	90.0	50.0	80.0	14.8	> 100	22.0	> 100	27.0	32.0	2.2	14.0	1.0	35.0	2.4	> 100	> 10
Metronidazole	1.1	0.4	25.0	1.1	18.3	6.4	9.1	2.7	> 100	> 10	> 100	> 10	> 100	> 10	> 100	> 10

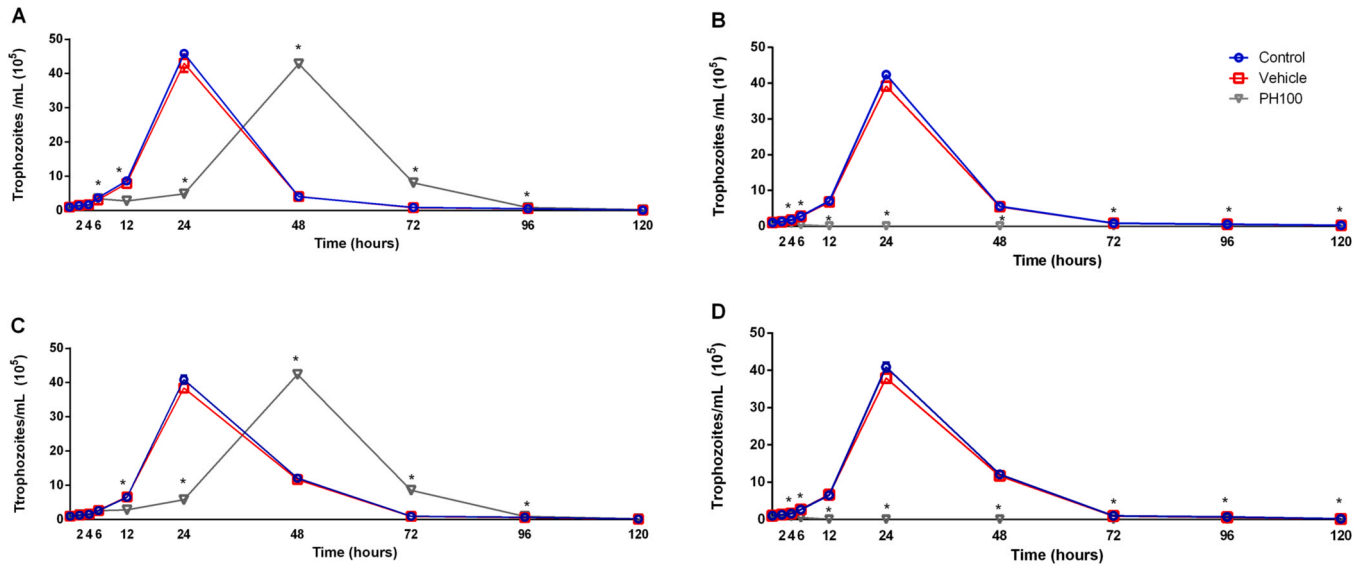

Fig. 1. Growth kinetics of PH100-treated trophozoites: (A) ATCC 30236 isolate at IC_{50} (50 μM); (B) ATCC 30236 isolate at MIC (90 μM); (C) TV-LACM15 clinical isolate at IC_{50} (14.8 μM); (D) TV-LACM15 clinical isolate at MIC (80 μM). (*) Statistically significant difference ($p < 0.05$) when compared to the negative control by the Student's *t*-test.

A

MTZ concentration (μM) \ PH100 concentration (μM)	3.70	7.40	14.80	29.60	59.20
0.28	2.97	3.23	2.55	2.57	1.01
0.55	2.68	2.35	2.38	2.43	0.79
1.10	2.53	2.36	1.96	0.96	0.61
2.20	1.88	1.14	0.91	0.68	0.46*
4.40	1.30	0.96	0.46*	0.38*	0.00*

B

MTZ concentration (μM) \ PH100 concentration (μM)	2.75	11.00	22.00	44.00	88.00
1.60	2.05	2.45	1.76	1.26	10.90
3.20	0.98	1.02	1.16	1.10	8.49
6.40	0.55	0.54	0.53	0.64	8.04
12.80	1.76	1.59	0.56	0.34*	0.00*
25.60	0.00*	0.00*	0.00*	0.00*	0.00*

C

MTZ concentration (μM) \ PH100 concentration (μM)	6.75	13.50	27.00	54.00	108.00
0.68	2.45	2.03	1.80	1.62	1.56
1.35	1.47	1.89	1.80	1.52	1.71
2.70	1.07	0.85	0.96	0.76	1.57
5.40	0.33*	0.36*	0.44*	0.44*	0.45*
10.80	0.34*	0.44*	0.16*	0.28*	0.21*

Synergism
No Interaction
Antagonism

Fig. 2. FICI data for *T. vaginalis* for each combination tested of PH100 and metronidazole. (A) TV-LACM15 isolate; (B) TV-LACM22 isolate; (C) TV-LACH4 isolate. The interaction was classified as 'synergy' if FICI ≤ 0.5, 'no interaction' if FICI $= 0.5$–4.0 and 'antagonism' if FICI > 4.0 (Odds et al., 2003). *Statistically significant with at least $p < 0.05$ compared to control (untreated trophozoites).

like (TvCP2) and calpain-like were decreased for both isolates. Interestingly, the gene expression of aminophospholipid translocase (APLT-1), an enzyme directly associated to apoptosis, was different for isolates, with a significant decrease for ATCC 30236 and increase for TV-LACM15. These results indicate that the treatment with PH100 modulates gene expression related to apoptosis-like cell death in *T. vaginalis* and reveal distinguished profiles between isolates.

3.8. PH100 induced morphological alterations

The *T. vaginalis* ATCC 30236 isolate morphology was evaluated after incubation with PH100 at IC_{50} (50 μM) for 24 h and compared to untreated parasites. As shown in Fig. 5, untreated parasites presented normal pyriform shape with characteristic features, undulating membrane (UM), free anterior flagella (AF), and axostyle (AX) (Fig. 5A). In contrast, PH100-treated parasites revealed alterations in the shape evidenced by the rounded form and internalization of flagella (Fig. 5B,D), with formation of blebbing (Fig. 5B). In addition, endoflagellar or pseudocyst forms (Fig. 5E), commonly found under stressful conditions, were also observed.

3.9. PH100 modulated peptidase activity

Azocasein assay showed that ATCC 30236 and TV-LACM15

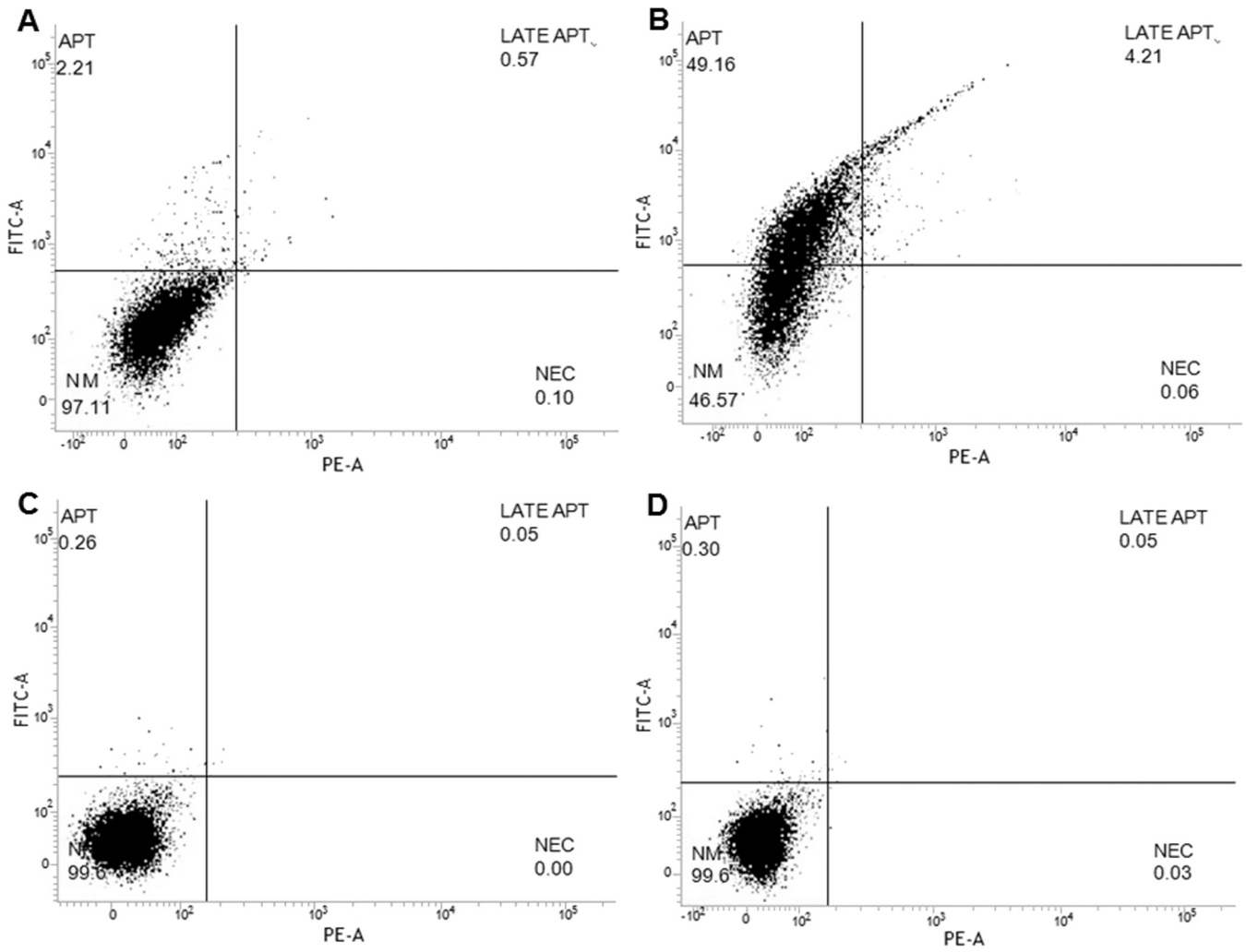

Fig. 3. Effect of PH100 on *T. vaginalis* suggesting apoptosis-like cell death. (A) ATCC 30236 isolate without treatment; (B) ATCC 30236 isolate treated with PH100 at IC_{50} (50 μM); (C) TV-LACM15 clinical fresh isolate without treatment; (D) TV-LACM15 clinical fresh isolate treated with PH100 at IC_{50} (14.8 μM). Data are representative of four different experiments (n = 4).

Table 2
Comparison of cell death events including apoptosis, late apoptosis, necrosis, normal morphology, and granularity (FSC and SSC) by flow cytometry analysis of *T. vaginalis* treated or not with PH100.

Cell death event (%)	ATCC 30236 Control	ATCC 30236 PH100	TV-LACM15 Control	TV-LACM15 PH100
Normal morphology	96.50 ± 2.58	45.91 ± 1.77	99.45 ± 0,25	99.45 ± 0.25
Apoptosis	2.19 ± 1.69	40.80 ± 7.70*	0.39 ± 0.16	0.38 ± 0.12
Late apoptosis	0.98 ± 0.82	12.16 ± 6.88	0.10 ± 0.04	0.06 ± 0.02
Necrosis	0.32 ± 0.17	1.14 ± 1.05	0.03 ± 0,06	0.05 ± 0.04
FSC[A]	32.60 ± 1.48	86.26 ± 9.7*	28.67 ± 2.37	36.34 ± 1.25
SSC[A]	65.90 ± 2.3	89.90 ± 7.00*	58.94 ± 1.23	64.68 ± 0.87

[A]Forward-angle light scatter (FSC) and side scatter (SSC) means of trophozoites treated and or not with PH100 at IC_{50}. *Statistically significant with at least $p < 0.05$ compared to control (untreated trophozoites).

trophozoites treatment with PH100 at IC_{50} (50 and 14.8 μM, respectively) decreased peptidases activity (60%) when compared with control (Supplemental Fig. S7).

3.10. Identification of peptidases possibly modulated by PH100 by a proteomic approach

The zymogram regions positively or negatively modulated by the PH100 were excised and analyzed by mass spectrometry (Supplemental Fig. S8). The protein identification was performed using *T. vaginalis* G3 genome data available at GeneBank. Focusing on peptidases that could be possible targets of PH100, two regions of the zymogram were analyzed. At the negatively (inhibited) modulated peptidase regions for ATCC 30236 isolate (Fig. S8 region a) we identified peptides belonging to GP63-like and ubiquitin hydrolase-like cysteine peptidases. At the positively modulated (activated) peptidase region for TV-LACM15 (Fig. S8 region b) we identified peptides belonging to GP63-like, ubiquitin hydrolase-like cysteine peptidase, leishmanolysin-like metallopeptidase, subtilisin-like serine peptidase, calpain catalytic domain-containing protein, and aminopeptidase P-like metallopeptidase

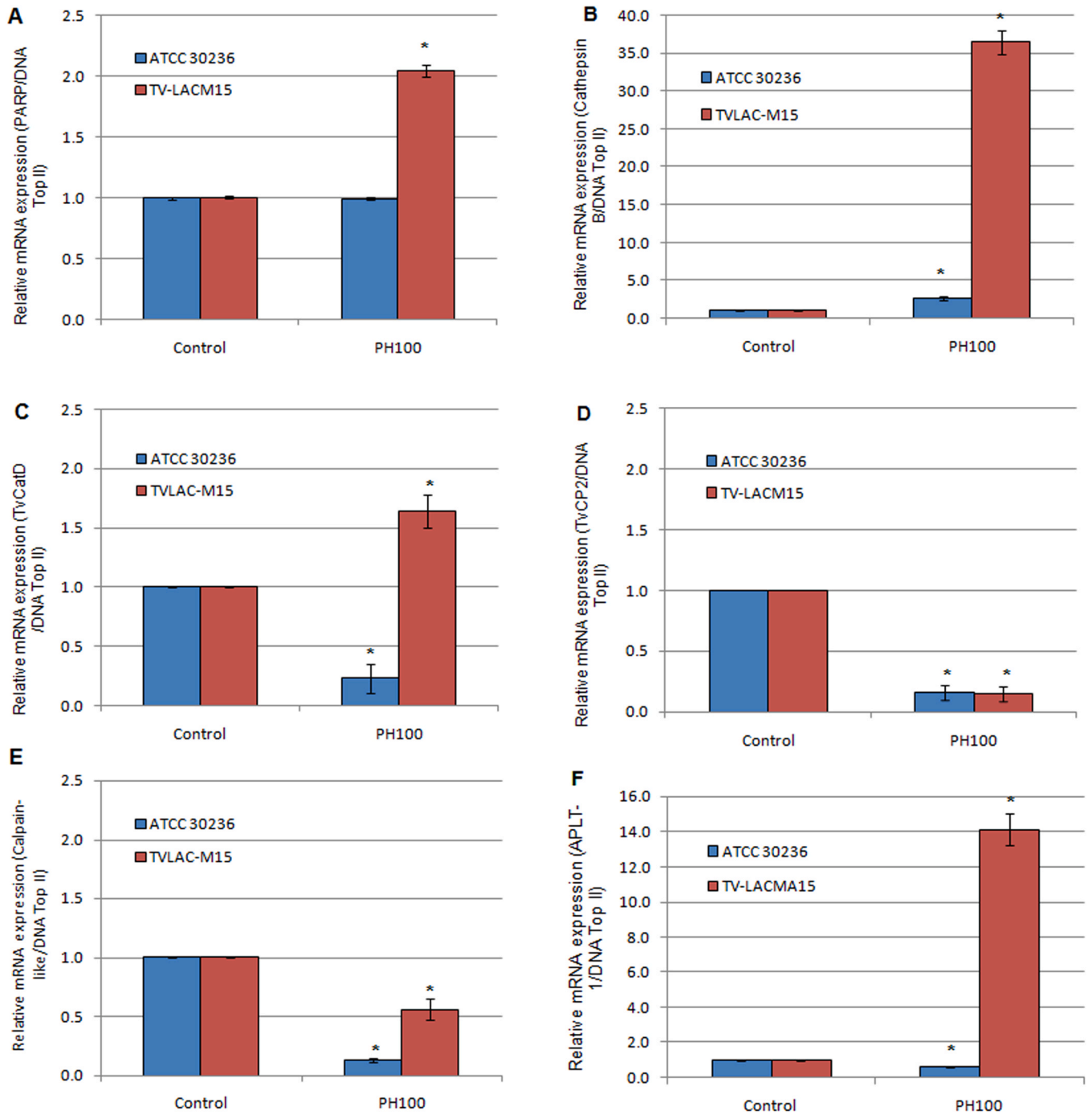

Fig. 4. Gene expression of *T. vaginalis* enzymes possibly involved in apoptosis-like cell death. The ATCC 30236 and TV-LACM15 isolates were treated or not with PH100 at IC50 (50 μM and 14.8 μM, respectively). (A) PARP; (B) Cathepsin B-like; (C) TvCatD; (D) TvCP2; (E) Calpain-like; (F) APLT-1. (*) Statistically significant difference ($p < 0.05$) when compared to the negative control by the Student's *t*-test.

pedptidases (Table 3).

4. Discussion

Studies have shown that derivatives of quinazoline are cytotoxic against protozoa with mechanisms of inhibition of dihydrofolate reductase in *Trypanosoma cruzi*, *Leishmania major,* and *Plasmodium vivax* [16] and modification of the *Toxoplasma gondii* structure preventing its entry in host cells [33]. In the present study we showed that 2,4-diamine-quinazoline derivative (PH100) kills *T. vaginalis*. The compound PH100 was tested against ATCC 30236 and three fresh clinical *T. vaginalis* isolates that presents different occurrences of symbiosis infections with *Mycoplasma hominis* and *Trichomonas virus* species (TVV) [34]. TVV are linear double-stranded RNA viruses observed in the trichomonads cytosol, divided in four viral species based on genomic sequences: TVV1, TVV2, TVV3, and TVV4, that can coexist or not in the same organism [35]. *T. vaginalis* virulence can be affected by TVV, such as the ability to evade the host immune defenses [36]. PH100 showed the best results for ATCC 30236 and TV-LACM15 isolates with IC_{50} values of 50 μM and 14.8 μM, respectively. In addition, when tested against the fresh clinical isolates TV-LACM22 (with no TVV but harboring *M. hominis*) and TV-LACH4 (harboring all TVV 1, 2, 3, and 4),

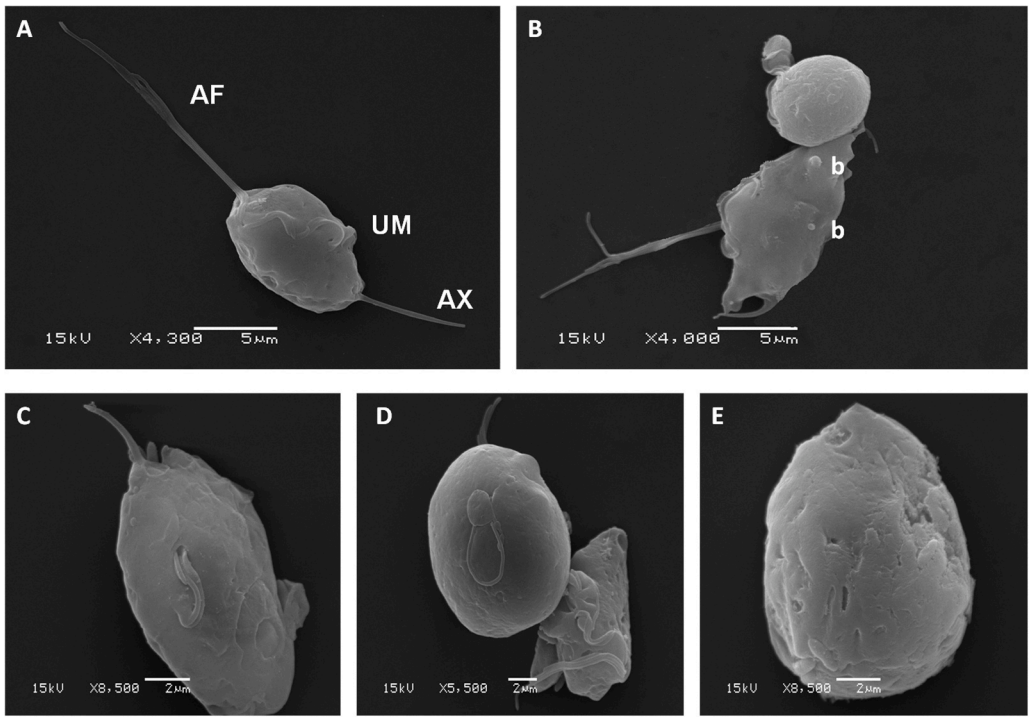

Fig. 5. Scanning electron microscopy of ATCC 30236 *T. vaginalis* isolate treated or not with PH100. (A) *T. vaginalis* with no treatment presented normal morphology: (AF) four anterior flagella, (UM) undulating membrane and (AX) axostyle. (B–E) *T. vaginalis* after treatment with PH100 at IC_{50} (50 µM) for 24 h. (B) An endoflagellar or pseudocyst form and a trophozoites showing blebbing (represented with b) or protrusions of the membrane; (C and D) Trophozoites initiating the internalization of flagella and alteration of the pyriform to the endoflagellar shape; (E) a characteristic endoflagellar form or pseudocyst, with all flagella internalized.

Table 3
Identified peptidases in excised regions "a" (ATCC 30236) and "b" (TV-LACM15) of zymogram by mass spectrometry.

Protein entry	Uniprot ID
	Region a
A2EJ58	GP63-like
A2D839	GP63-like
A2E849	Clan CA, family C19, ubiquitin hydrolase-like cysteine peptidase
A2EDA7	Clan CA, family C19, ubiquitin hydrolase-like cysteine peptidase
A2DZK1	Clan CA, family C19, ubiquitin hydrolase-like cysteine peptidase
A2FXH1	Clan CA, family C19, ubiquitin hydrolase-like cysteine peptidase
A2EZM1	Clan CA, family C19, ubiquitin hydrolase-like cysteine peptidase
A2EM39	Clan CA, family C19, ubiquitin hydrolase-like cysteine peptidase
A2DUQ7	Clan CA, family C19, ubiquitin hydrolase-like cysteine peptidase
	Region b
A2E5S6	GP63-like
A2G9D4	GP63-like
A2FTN8	Clan MA, family M8, leishmanolysin-like metallopeptidase
A2E0B6	Clan SB, family S8, subtilisin-like serine peptidase
A2DDC2	Calpain catalytic domain-containing protein
A2DYZ1	Clan MG, family M24, aminopeptidase P-like metallopeptidase
A2EDA7	Clan CA, family C19, ubiquitin hydrolase-like cysteine peptidase
A2EJI5	Clan CA, family C19, ubiquitin hydrolase-like cysteine peptidase
A2G0N3	Clan CA, family C19, ubiquitin hydrolase-like cysteine peptidase
A2FDH2	Clan CA, family C19, ubiquitin hydrolase-like cysteine peptidase
A2EZM1	Clan CA, family C19, ubiquitin hydrolase-like cysteine peptidase
A2EM39	Clan CA, family C19, ubiquitin hydrolase-like cysteine peptidase
A2F7×4	Clan CA, family C19, ubiquitin hydrolase-like cysteine peptidase
A2F894	Clan CA, family C19, ubiquitin hydrolase-like cysteine peptidase
A2F763	Clan CA, family C19, ubiquitin hydrolase-like cysteine peptidase

PH100 showed IC_{50} values higher than that for TV-LACM15 (with no TVV neither *M. hominis*). These differences of values can be related to the presence of endosymbionts TVV that upregulates the expression of cysteine peptidases involved in virulence factors such as cytoadherence, cytotoxicity, and host immune evasion [37]. This issue should be further explored by testing PH100 effect in a higher number of *T. vaginalis* isolates with different profiles of TVV harboring since the commensal relationship between *T. vaginalis* and TVV impairs the experimental infection and/or removal of TVV [38].

Moreover, the checkerboard results demonstrated a synergistic effect upon the association of metronidazole and PH100. Based on the results obtained, we can suggest further studies involving the use of both compounds because the combination of concentrations that showed a synergistic effect for all *T. vaginalis* clinical isolates tested in this study allow a reduction in the used concentration of PH100 (from the IC_{50} with metronidazole IC_{50} X4), thus assisting in the elimination of infections by metronidazole resistant-isolates due to the distinct mechanisms of action.

In addition, the type of cell death caused by the PH100 activity was investigated. Annexin V conjugated with FITC binds to phosphatidylserine exposed on plasmatic membrane and propidium iodide detects dead cells. The ATCC 30236 isolate showed fluorescent unities in characteristic regions and these data associated with the type of cytoplasmic granules and membrane roughness (increase in granularity and cell internal complexity) suggest morphological changes indicative of apoptosis-like cell death. Conversely, PH100-treated TV-LACM15 trichomonads did not present fluorescence, showing cell death without apoptosis features. This intriguing result revealed distinct findings in cell death profiles between the ATCC and fresh clinical *T. vaginalis* isolates. Apoptosis-like programmed cell death (PCD) in protozoan parasites shares some morphological features with PCD in multicellular organisms. However, both the evolutionary explanations and mechanisms involved in parasite PCD are poorly understood [39].

Scanning electron microscopy revealed alterations in *T. vaginalis* morphology from characteristic pyriform to pseudocyst formation with internalization of flagella. This shape is commonly observed in response to stress conditions as nutrient depletion and presence of drugs [40]. Additional morphological changes could be observed, with formation of blebbing, cellular membrane protrusions commonly associated with apoptosis [41]. These results corroborate to Annexin V positive for ATCC 30236 isolate, suggesting apoptosis-like as mechanism of action of PH100 for the long-term-grown isolate.

In order to investigate the mechanism of cell death and differences between ATCC and fresh clinical *T. vaginalis* isolate (TV-LACM15), the gene expression of enzymes with function involved in the apoptosis process described in evolutionary related organisms was analyzed. Table 4 shows the functions of each enzyme evaluated, relationship of gene expression to apoptosis, and gene modulation results generated by

Table 4
Gene expression of enzymes in *T. vaginalis* isolates (ATCC 30236 and TV-LACM15) treated with PH100 at IC_{50} for 24 h and function of enzymes and relation of expression and apoptosis.

Enzyme	Function	Expression/Apoptosis	mRNA expression with PH100 treatment	
			ATCC 30236	TV-LACM15
Poly [ADP-Ribose] Polymerase	DNA repair, transcription, cell cycle, cell death and genomic integrity (Cao et al., 2019).	Reduced gene expression = Increases apoptosis	N.A.	Increased
Cathepsin D-like	Protein catabolism; Stimulates proliferation cancer cells (Bach et al., 2015).	Reduced gene expression = Increases apoptosis	Reduced	Increased
Cathepsin B-like	Turnover of intracellular and extracellular proteins; Play an important role in apoptosis degrading a number of anti-apoptotic proteins (Cavallo-Medvet et al., 2011).	Increased gene expression = Increases apoptosis	Increased	Increased
Cathepsin L-like	Initiation of protein degradation/Turnover of intracellular and extracellular proteins (Sui et al., 2016).	Increased gene expression = Increases apoptosis	Reduced	Reduced
Calpain	Cell differentiation, proliferation and death (Liu et al., 2019).	Increased gene expression = Increases apoptosis	Reduced	Reduced
Aminophospholipid translocase (APLT-1)	Responsible for the sequestration of phosphatidylserine in the cytosolic leaflet of plasma membranes (Dolis et al., 1997).	Reduced gene expression = Increases apoptosis	Reduced	Increased

N.A. = not altered.

treatment with PH100 in each *T. vaginalis* isolate. Our data show that the gene expressions of TvCatD, cathepsin B-like, and APLT-1 were decreased in the ATCC isolate after PH100 treatment, corroborating with Annexin V and scanning electron microscopy results and indicating relation with apoptosis-like cell death type. In contrast, TvCatD and APLT-1 gene expressions were increased in the TV-LACM15 fresh clinical isolate, suggesting that the cell death type elicited by the compound is not apoptosis-like in this isolate. Table 5 shows the comparison between both isolates and features related or not to apoptosis-like. Moreover, theoretically, alterations in gene expression can lead to altered protein levels, but the still unknown steps between transcription and translation provide many different regulatory processes. Molecules trigger intercellular signaling cascades that cause changes in transcription or expression of genes. Such changes in gene expression can include turnover of genes or just slightly adjust the level of transcript produced [42]. Therefore, transcription analysis by gene expression themselves are not sufficient to predict protein levels and further detection using specific antibodies are necessary [43].

Peptidases are enzymes responsible for protein cleavage and therefore, potential drug targets. *T. vaginalis* has about 440 genes encoding peptidases: 220 cysteine-like (CP), 123 metallo-like (MP), 80 serine (SP), 17 threonine (TP), and 6 aspartic peptidases (AP) [44]. Peptidases act as virulence factors in trichomoniasis and may be located on the surface of the plasma membrane or secreted [45]. Results presented in this study show that PH100 modulates the expression of enzymes, including peptidases. Therefore, azocasein assay was performed to investigate the effect of the compound on the activity of peptidases. Reduction (60%) in total peptidase activity was observed for both PH100-treated isolates. In order to identify which peptidases had activities modified by the treatment, zymograms and mass spectrometry were made. Modifications were possible to be observed in peptidase activity from the gel regions analyzed, comparing trophozoites treated or not with PH100 at IC_{50} for 24 h. The regions that showed differences in the SDS-PAGE were excised and analyzed by mass spectrometry. The analysis showed two peptidases presented on the region with decreased activity excised from ATCC isolate, GP63-like and ubiquitin hydrolase-like cysteine peptidase, and six peptidases presented on the region with increased activity excised from TV-LACM15, GP63-like, ubiquitin hydrolase-like cysteine peptidase, leishmanolysin-like metallopeptidase, subtilisin-like serine peptidase, calpain catalytic domain-containing protein, and aminopeptidase P-like metallopeptidase. Taking into account the correlation between gene expression data with mass spectrometry analysis it can be suggested that the derivative PH100 modulates both peptidases gene expression and activity.

Table 5
Comparison between PH100-treated isolates and features related or not to apoptosis-like.

	ATCC 30236	TV-LACM15
Annexin V - FITC	Phosphatidylserine exposed	Phosphatidylserine not exposed
Scanning Electron Microscopy	Pseudocyst formation and blebbing	N.D.
PCR	Gene expression favors apoptosis	Gene expression favors DNA repair
Mass Spectrometry	Ubiquitin hydrolase-like cysteine peptidase decreased activity	Ubiquitin hydrolase-like cysteine peptidase increased activity
Characteristics of apoptosis-like	Yes	No

GP63-like, aminopeptidase P-like metallopeptidase (TvMP50), leishmanolysin-like metallopeptidase, calpain catalytic domain-containing protein and subtilisin-like serine peptidase are responsible to *T. vaginalis* virulence, migration, invasion, and cytoadhesion [46–49]. One hypothesis to explain the augment of the activity of these enzymes is the attempt of the parasite to overcome the stressful exposition to PH100 by eliciting some virulence factors.

Thereby, ubiquitination plays important role on cell death, marking proteins for degradation [50]. Ubiquitin hydrolases are members of desubiquitination family that has been identified in the mammalian genome [51]. Deubiquitinating process is not completely understood; however, recent studies showed deubiquitinating enzymes have important role on regulation of cell cycle, gene expression, DNA repair, prevention of protein degradation, and promoting or inhibiting apoptosis in mammalian cells [50]. However, there are no studies on the function of ubiquitin hydrolyses in *T. vaginalis*. Analyzing the results obtained for the PH100-treated isolates, the ubiquitin hydrolase-like cysteine peptidase, increased on TV-LACM15 and decreased on ATCC 30236 isolate, appears to provide protection against apoptosis with an anti-apoptotic function.

5. Conclusions

Overall, this study revealed that 2,4-diamine-quinazoline derivative (PH100) kills *T. vaginalis* through a mechanism of action that is poorly understood for this parasite. The trichomonacidal activity was more effective against the fresh clinical isolate less metronidazole-susceptible and a synergistic effect upon the association with metronidazole was found. The differential susceptibility to PH100 may be related to the presence of endosymbionts TVV. Altogether, the results demonstrated by morphological analysis, gene expression and proteomic approach

revealed that PH100 kills *T. vaginalis* by modulating peptidases triggering apoptosis-like cell death only in the ATCC isolate, revealing heterogeneity regarding cell death type elicitedś.

Funding

This work was supported by Conselho Nacional de Desenvolvimento Científico e Tecnológico (CNPq, Brazil) grants 428538/2018-5 (TT) and 402318/2016-1 (SFA), Fundação de Amparo à Pesquisa do Estado do Rio Grande do Sul (FAPERGS/PRONEM, Brazil) grant 16/2551-0000244-4, and by the Coordenação de Aperfeiçoamento de Pessoal de Nível Superior (CAPES, Brazil) Finance Code 001. JIW is thankful to CAPES (Brazil) for a master in science fellowship (grant 345887/2019-1). TT thanks CNPq for researcher fellowship (grant 312292/2017-1).

Acknowledgements

The valuable discussion on zymograms technical development is acknowledged to Professor Lucélia Santi, Faculdade de Farmácia, UFRGS. The authors thank Centro de Microscopia e Microanálise (CMM/UFRGS) for technical assistance.

Conflict of interest statement

The authors declare no conflict of interest.

Appendix A. Supporting information

Supplementary data associated with this article can be found in the online version at doi:10.1016/j.biopha.2021.111611.

References

[1] M.M. Hobbs, A.C. Seña, Modern diagnosis of *Trichomonas vaginalis* infection, Sex. Transm. Infect. 89 (6) (2013) 434–438, https://doi.org/10.1136/sextrans-2013-051057.

[2] W.E. Secor, E. Meites, M.C. Starr, K.A. Workowski, Neglected parasitic infections in the United States: trichomoniasis, Am. J. Trop. Med. Hyg. 90 (5) (2014) 800–804, https://doi.org/10.4269/ajtmh.13-0723.

[3] J. Rowley, S.V. Hoorn, E. Korenromp, N. Low, M. Unemo, L.J. Abu-Raddad, R. M. Chico, A. Smolak, L. Newman, S. Gottlieb, S.S. Thwin, N. Broutet, M.M. Taylor, Chlamydia, gonorrhoea, trichomoniasis and syphilis: global prevalence and incidence estimates, 2016, Bull. World Health Organ. 97 (8) (2019) 548–562, https://doi.org/10.2471/blt.18.228486.

[4] D.N. Poole, R.S. McClelland, Global epidemiology of *Trichomonas vaginalis*, Sex. Transm. Infect. 89 (6) (2013) 418–422, https://doi.org/10.1136/sextrans-2013-051075.

[5] R.P. Hirt, J. Sherrard, *Trichomonas vaginalis* origins, molecular pathobiology and clinical considerations, Curr. Opin. Infect. Dis. 28 (1) (2015) 72–79, https://doi.org/10.1097/qco.0000000000000128.

[6] P. Kissinger, *Trichomonas vaginalis*: a review of epidemiologic, clinical and treatment issues, BMC Infect. Dis. 15 (2015) 307, https://doi.org/10.1186/s12879-015-1055-0.

[7] C.B. Menezes, A.P. Frasson, T. Tasca, Trichomoniasis – are we giving the deserved attention to the most common non-viral sexually transmitted disease worldwide? Microb. Cell 3 (9) (2016) 404–419, https://doi.org/10.15698/mic2016.09.526.

[8] P.B. Vieira, T. Tasca, W.E. Secor, Challenges and persistent questions in the treatment of Trichomoniasis, Curr. Top. Med. Chem. 17 (11) (2017) 1249–1265, https://doi.org/10.2174/1568026616666160930150429.

[9] J.R. Schwebke, F.J. Barrientes, Prevalence of *Trichomonas vaginalis* isolates with resistance to metronidazole and tinidazole, Antimicrob. Chemother. 50 (12) (2006) 4209–4210, https://doi.org/10.1128/aac.00814-06.

[10] R.D. Kirkcaldy, P. Augostini, L.E. Asbel, K.T. Bernstein, R.P. Kerani, C. J. Mettenbrink, P. Pathela, J.R. Schwebke, W.E. Secor, K.A. Workowski, D. Davis, J. Braxton, H.S. Weinstock, *Trichomonas vaginalis* antimicrobial drug resistance in 6 US cities, STD Surveillance Network, 2009-2010, Emerg. Infect. Dis. 18 (6) (2012) 939–943, https://doi.org/10.3201/eid1806.111590.

[11] S. Ravez, O. Castillo-Aguilera, P. Depreux, L. Goossens, Quinazoline derivatives as anticancer drugs: a patent review (2011–present), Expert Opin. Ther. 25 (7) (2015) 789–804, https://doi.org/10.1517/13543776.2015.1039512.

[12] H.A. Abuelizz, A.E. Hassane, M. Marzouk, E. Ezzeldin, A.A. Ali, R. Al-Salahi, Molecular modeling, enzyme activity, anti-inflammatory and antiarthritic activities of newly synthesized quinazoline derivatives, Future Med. Chem. 9 (17) (2017) 1995–2009, https://doi.org/10.4155/fmc-2017-0157.

[13] M. Zeng, J. Lu, L. Li, F. Feru, C. Quan, T.W. Gero, S.B. Ficarro, Y. Xiong, C. Ambrogio, R.M. Paranal, M. Catalano, J. Shao, K.K. Wong, J.A. Marto, E. S. Fischer, P.A. Jänne, D.A. Scott, K.D. Westover, N.S. Gray, Potent and selective covalent quinazoline inhibitors of KRAS G12C, Cell Chem. Biol. 24 (8) (2017) 1005–1016, https://doi.org/10.1016/j.chembiol.2017.06.017.

[14] S. Kant, S. Asthana, D. Missiakas, V. Pancholi, A novel STK1-targeted small-molecule as an "antibiotic resistance breaker" against multidrug-resistant *Staphylococcus aureus*, Sci. Rep. 7 (1) (2017) 5067, https://doi.org/10.1038/s41598-017-05314-z.

[15] S.V. dos Reis, N.S. Ribeiro, D.A. Rocha, I.S. Fortes, D.S. Trentin, S.F. Andrade, A. J. Macedo, N 4 -benzyl-N 2 -phenylquinazoline-2,4-diamine compound presents antibacterial and antibiofilm effect against *Staphylococcus aureus* and *Staphylococcus epidermidis*, Chem. Biol. Drug Des. 96 (6) (2020) 1372–1379, https://doi.org/10.1111/cbdd.13745.

[16] C. Mendoza-Martínez, J. Correa-Basurto, R. Nieto-Meneses, A. Márquez-Navarro, R. Aguilar-Suárez, M.D. Montero-Cortes, B. Nogueda-Torres, E. Suárez-Contreras, N. Galindo-Sevilla, A. Rojas-Rojas, A. Rodriguez-Lezama, A. Rodriguez-Lezama, Design, synthesis and biological evaluation of quinazoline derivatives as anti-trypanosomatid and anti-plasmodial agents, Eur. J. Med. Chem. 96 (2015) 296–307, https://doi.org/10.1016/j.ejmech.2015.04.028.

[17] A. Gellis, N. Primas, S. Hutter, V. Remusat, P. Verhaeghe, P. Vanelle, N. Azas, Looking for new antiplasmodial quinazolines: DMAP-catalyzed synthesis of 4-benzyloxy-and 4-aryloxy-2-trichloromethylquinazolines and their in vitro evaluation toward *Plasmodium falciparum*, Eur. J. Med. Chem. 119 (2016) 34–44, https://doi.org/10.1016/j.ejmech.2016.04.059.

[18] Z. Li, B. Wang, J.Q. Hou, S.L. Huang, T.M. Ou, J.H. Tan, L.K. An, D. Li, L.Q. Gu, Z. S. Huang, 2-(2-indolyl-)-4 (3H)-quinazolines derivates as new inhibitors of AChE: design, synthesis, biological evaluation and molecular modelling, J. Enzym. Inhib. Med. Chem. 28 (3) (2013) 583–592, https://doi.org/10.3109/14756366.2012.663363.

[19] B. Tang, M. Wei, Q. Niu, Y. Huang, S. Ru, X. Liu, L. Shen, Q. Fang, Antimicrobial activity of quinazolin derivatives of 1, 2-Di (quinazolin-4-yl) diselane against Mycobacteria, BioMed Res. 2017 (2017), 5791781, https://doi.org/10.1155/2017/5791781.

[20] M.K. Ibrahim, I.H. Eissa, M.S. Alesawy, A.M. Metwaly, M.M. Radwan, M. A. ElSohly, Design, synthesis, molecular modeling and anti-hyperglycemic evaluation of quinazolin-4 (3H)-one derivatives as potential PPARγ and SUR agonists, Bioorg. Med. Chem. 25 (17) (2017) 4723–4744, https://doi.org/10.1016/j.bmc.2017.07.015.

[21] H.A. Abuelizz, R.E. Dib, M. Marzouk, E.H. Anouar, Y. A Maklad, H. N Attia, R. Al-Salahi, Molecular docking and anticonvulsant activity of newly synthesized quinazoline derivatives, Molecules 22 (7) (2017) 1094, https://doi.org/10.3390/molecules22071094.

[22] M. Dukat, K. Alix, J. Worsham, S. Khatri, M.K. Schulte, 2-Amino-6-chloro-3, 4-dihydroquinazoline: a novel 5-HT3 receptor antagonist with antidepressant character, Bioorg. Med. Chem. Lett. 23 (21) (2013) 5945–5948, https://doi.org/10.1016/j.bmcl.2013.08.072.

[23] S.R. Pathak, V. Malhotra, R. Nath, K. Shanker, Synthesis and antihypertensive activity of novel quinazolin-4 (3H)-one derivatives, Cent. Nerv. Syst. Agents Med. Chem. Former. Curr. Med. Cent. Nerv. Syst. Agents 14 (1) (2014) 34–38, https://doi.org/10.2174/18715249146661408251447 29.

[24] L.S. Diamond, The establishment of various trichomonads of animals and man in axenic cultures, Int. J. Parasitol. 43 (4) (1957) 488–490.

[25] D.P.G. Hübner, P.B. Vieira, A.P. Frasson, C.B. Menezes, F.R. Senger, G.N. Santos da Silva, S.C.B. Gnoatto, T. Tasca, Anti-Trichomonas vaginalis activity of betulinic acid derivatives, Biomed. Pharmacother. 84 (2016) 476–484, https://doi.org/10.1016/j.biopha.2016.09.064.

[26] T. Kiss, F. Fenyvesi, I. Bácskay, J. Váradi, E. Fenyvesi, R. Iványi, L. Szente, A. Tósaki, M. Vecsernyés, Evaluation of the cytotoxicity of β-cyclodextrin derivatives: evidence for the role of cholesterol extraction, Eur. J. Pharm. Sci. 40 (4) (2010) 376–380, https://doi.org/10.1016/j.ejps.2010.04.014.

[27] F.C. Odds, Synergy, antagonism, and what the chequerboard puts between them, J. Antimicrob. Chemother. 52 (1) (2003) 1, https://doi.org/10.1093/jac/dkg301.

[28] N. Mallo, J. Lamas, J.M. Leiro, Hydrogenosome metabolism is the key target for antiparasitic activity of resveratrol against *Trichomonas vaginalis*, Antimicrob. Agents Chemother. 57 (6) (2013) 2476–2484, https://doi.org/10.1128/aac.00009-13.

[29] M.P. Thomé, E.C. Filippi-Chiela, E.S. Villodre, C.B. Migliavaca, G.R. Onzi, K. B. Felipe, G. Lenz, Ratiometric analysis of Acridine Orange staining in the study of acidic organelles and autophagy, J. Cell Sci. 129 (24) (2016) 4622–4632, https://doi.org/10.1242/jcs.195057.

[30] O. Santos, G.V. Rigo, A.P. Frasson, A.J. Macedo, T. Tasca, Optimal reference genes for gene expression normalization in *Trichomonas vaginalis*, PLoS One 10 (9) (2015), 0138331, https://doi.org/10.1371/journal.pone.0138331.

[31] M.M. Bradford, A rapid and sensitive method for the quantitation of microgram quantities of protein utilizing the principle of protein-dye binding, Anal. Biochem. 72 (1976) 248–254, https://doi.org/10.1006/abio.1976.9999.

[32] J.M. Carlton, R.P. Hirt, J.C. Silva, A.L. Delcher, M. Schatz, Q. Zhao, J.R. Wortman, S.L. Bidwell, U.C. Alsmark, S. Besteiro, T. Sicheritz-Ponten, C.J. Noel, J.B. Dacks, P. G. Foster, C. Simillion, Y. Van de Peer, D. Miranda-Saavedra, G.J. Barton, G. D. Westrop, S. Müller, D. Dessi, P.L. Fiori, Q. Ren, I. Paulsen, H. Zhang, F. D. Bastida-Corcuera, A. Simoes-Barbosa, M.T. Brown, R.D. Hayes, M. Mukherjee, C. Y. Okumura, R. Schneider, A.J. Smith, S. Vanacova, M. Villalvazo, B.J. Haas, M. Pertea, T.V. Feldblyum, T.R. Utterback, C.L. Shu, K. Osoegawa, P.J. de Jong, I. Hrdy, L. Horvathova, Z. Zubacova, P. Dolezal, S.B. Malik, J.M. Jr Logsdon, K. Henze, A. Gupta, C.C. Wang, R.L. Dunne, J.A. Upcroft, P. Upcroft, O. White, S. L. Salzberg, P. Tang, C.H. Chiu, Y.S. Lee, T.M. Embley, G.H. Coombs, J.C. Mottram, J. Tachezy, C.M. Fraser-Liggett, P.J. Johnson, Draft genome sequence of the

sexually transmitted pathogen *Trichomonas vaginalis*, Science 315 (5809) (2007) 207–212, https://doi.org/10.1126/science.1132894.
[33] A.A. El-Tombary, K.A. Ismail, O.M. Aboulwafa, A.M.M. Omar, M.Z. El-Azzouni, S. T. El-Mansoury, Novel triazolo [4, 3-a] quinazolinone and bis-triazolo [4, 3-a: 4, 3′-c] quinazolines: synthesis and antitoxoplasmosis effect, Il Farmaco 54 (7) (1999) 486–495, https://doi.org/10.1016/s0014-827x(99)00038-5.
[34] D.L. Becker, O. dos Santos, A.P. Frasson, G. de Vargas Rigo, A.J. Macedo, T. Tasca, High rates of double-stranded RNA viruses and *Mycoplasma hominis* in *Trichomonas vaginalis* clinical isolates in South Brazil, Infect. Genet. Evol. 34 (2015) 181–187, https://doi.org/10.1016/j.meegid.2015.07.005.
[35] R.P. Goodman, S.A. Ghabrial, R.N. Fichorova, M.L. Nibert, Trichomonasvirus: a new genus of protozoan viruses in the family *Totiviridae*, Arch. Virol. 156 (1) (2011) 171–179, https://doi.org/10.1007/s00705-010-0832-8.
[36] R. Fichorova, J. Fraga, P. Rappelli, P.L. Fiori, *Trichomonas vaginalis* infection in symbiosis with *Trichomonasvirus* and *Mycoplasma*, Res. Microbiol. 168 (9–10) (2017) 882–891, https://doi.org/10.1016/j.resmic.2017.03.005.
[37] R.N. Fichorova, Y. Lee, H.S. Yamamoto, Y. Takagi, G.R. Hayes, R.P. Goodman, X. Chepa-Lotrea, O.R. Buck, R. Murray, T. Kula, D.H. Beach, B.N. Singh, M. L. Nibert, Endobiont viruses sensed by the human host–beyond conventional antiparasitic therapy, PLoS One 7 (11) (2012) 48418, https://doi.org/10.1371/journal.pone.0048418.
[38] K.J. Graves, A.P. Ghosh, N. Schmidt, P. Augostini, W.E. Secor, J.R. Schwebke, D. H. Martin, P.J. Kissinger, C.A. Muzny, *Trichomonas vaginalis* virus among women with Trichomoniasis and associations with demographics, clinical outcomes, and metronidazole resistance, Clin. Infect. Dis. 69 (12) (2019) 2170–2176, https://doi.org/10.1093/cid/ciz146.
[39] S. Kaczanowski, M. Sajid, S.E. Reece, Evolution of apoptosis-like programmed cell death in unicellular protozoan parasites, Parasites Vectors 4 (2011) 44, https://doi.org/10.1186/1756-3305-4-44.
[40] M. Benchimol, Trichomonads under microscopy, Microsc. Microanal. 10 (5) (2004) 528–550, https://doi.org/10.1017/s1431927604040905.
[41] G.T. Charras, A short history of blebbing, J. Microsc. 231 (3) (2008) 466–478, https://doi.org/10.1111/j.1365-2818.2008.02059.x.
[42] A. Ralston, K. Shaw, Gene expression regulates cell differentiation, Nat. Educ. 1 (1) (2008) 127–131.
[43] Y. Liu, A. Beyer, R. Aebersold, On the dependency of cellular protein levels on mRNA abundance, Cell 165 (3) (2016) 535–550, https://doi.org/10.1016/j.cell.2016.03.014.
[44] R. Arroyo, R.E. Cárdenas-Guerra, E.E. Figueroa-Angulo, J. Puente-Rivera, O. Zamudio-Prieto, J. Ortega-López, *Trichomonas vaginalis* cysteine proteinases: iron response in gene expression and proteolytic activity, BioMed Res. Int. 2015 (2015), 946787, https://doi.org/10.1155/2015/946787.
[45] E.E. Figueroa-Angulo, F.J. Rendón-Gandarilla, J. Puente-Rivera, J.S. Calla-Choque, R.E. Cárdenas-Guerra, J. Ortega-López, L.I. Quintas-Granados, M.E. Alvarez-Sánchez, R. Arroyo, The effects of environmental factors on the virulence of *Trichomonas vaginalis*, Microbes Infect. 14 (15) (2012) 1411–1427, https://doi.org/10.1016/j.micinf.2012.09.004.
[46] M.D.C. Martínez-Herrero, M.M. Garijo-Toledo, F. González, I. Bilic, D. Liebhart, P. Ganas, M. Hess, M.T. Gómez-Muñoz, Membrane associated proteins of two *Trichomonas gallinae* clones vary with the virulence, PLoS One 14 (10) (2019), 0224032, https://doi.org/10.1371/journal.pone.0224032.
[47] J. Puente-Rivera, J.L. Villalpando, A. Villalobos-Osnaya, L.I. Vázquez-Carrillo, G. Léon-Ávila, M.D. Ponce-Regalado, C. López-Camarillo, J.M. Elizalde-Contreras, E. Ruiz-May, R. Arroyo, M.E. Alvarez-Sánchez, The 50kDa metalloproteinase TvMP50 is a zinc-mediated Trichomonas Vaginalis virulence factor, Mol. Biochem. Parasitol. 217 (2017) 32–41, https://doi.org/10.1016/j.molbiopara.2017.09.001.
[48] B. McHugh, S.A. Krause, B. Yu, A.M. Deans, S. Heasman, P. McLaughlin, M.M. S. Heck, Invadolysin: a novel, conserved metalloprotease links mitotic structural rearrangements with cell migration, J. Cell Biol. 167 (4) (2004) 673–686, https://doi.org/10.1083/jcb.200405155.
[49] P. Hernández-Romano, R. Hernández, R. Arroyo, J.F. Alderete, I. López-Villaseñor, Identification and characterization of a surface-associated, subtilisin-like serine protease in *Trichomonas vaginalis*, Parasitology 137 (11) (2010) 1621–1635, https://doi.org/10.1017/s003118201000051x.
[50] S. Ramakrishna, B. Suresh, K.H. Baek, The role of deubiquitinating enzymes in apoptosis, Cell. Mol. Life Sci. 68 (1) (2011) 15–26, https://doi.org/10.1007/s00018-010-0504-6.
[51] J. Kwon, Y.L. Wang, R. Setsuie, S. Sekiguchi, M. Sakurai, Y. Sato, W.W. Lee, Y. Ishii, S. Kyuwa, M. Noda, K. Wada, Y. Yoshikawa, Developmental regulation of ubiquitin C-terminal hydrolase isozyme expression during spermatogenesis in mice, Biol. Reprod. 71 (2) (2004) 515–521, https://doi.org/10.1095/biolreprod.104.027565.